

Electric Field and Potential Distributions along Non-Ceramic Insulators with Water Droplets

ABSTRACT

The electric field and potential distributions along wet non-ceramic insulators are calculated using COULOMB, a three-dimensional electric field analysis program. The electric field intensification on the surface of the water droplets on a flat hydrophobic silicone rubber (SIR) sheet is analyzed. The conductivity of the water droplets is also an important factor in the electric field intensification. Under rain or fog conditions, the potential distributions influenced by the water droplets on the weathershed of the insulator are calculated. The plots of equipotential lines for a few typical cases (modeling dry-and-clean, rain, and fog conditions) are also shown.

Integrated Engineering Software - Website Links

[Home](#)[Products](#)[Support](#)[Technical Papers](#)

"Page Down" or use scroll bars to read the article

Electric Field and Potential Distributions along Non-Ceramic Insulators with Water Droplets

Weiguo Que and Stephen A. Sebo
Department of Electrical Engineering
The Ohio State University
Columbus, Ohio 43210-1272, U.S.A

Abstract: The electric field and potential distributions along wet non-ceramic insulators are calculated using COULOMB, a three-dimensional electric field analysis program. The electric field intensification on the surface of the water droplets on a flat hydrophobic silicone rubber (SIR) sheet is analyzed. The conductivity of the water droplets is also an important factor in the electric field intensification. Under rain or fog conditions, the potential distributions influenced by the water droplets on the weathershed of the insulator are calculated. The plots of equipotential lines for a few typical cases (modeling dry-and-clean, rain, and fog conditions) are also shown.

INTRODUCTION

The pollution performance of non-ceramic insulators is well known. Due to the weak bonds of polymer materials, the non-ceramic insulators are more susceptible to chemical changes. During the service life of an insulator, the combined effects of electric and environmental stresses, such as the energizing voltage, maybe corona and arcing, also contamination, precipitation, ultraviolet rays, heat cycling, etc., might result in the slow degradation of some its insulating features. As a consequence, the hydrophobicity properties of the polymer weather shed will be temporarily or permanently lost. That might worsen the wet and contamination performance of non-ceramic insulators.

The pollution flashover phenomena of non-ceramic insulators have been studied and described by various researchers [1, 2]. The flashover of non-ceramic insulators during rain conditions shows that a discharge bridges the weather sheds and the leakage distance along the surface of the insulators is not used efficiently. The flashover of non-ceramic insulators with artificial contamination in clean fog tests shows that the discharges on a fully contaminated insulator follow the leakage path along the surface of the insulator. For partially contaminated insulators, the discharges in the contaminated section follow the leakage path along the surface of the insulator in the contaminated part. However, an arc develops and bridges the weather sheds along the clean section of the insulator which is a high resistance region. The presence of water droplets and contaminated layers intensify the electric field strength on the surface of a non-ceramic insulator. Therefore, the study of the electric and potential field distributions of non-ceramic insulators under wet and

contaminated conditions is important for the in-depth understanding of the initiation mechanism of pollution flashovers.

The water droplets play several roles in the pollution flashover and aging of non-ceramic insulators:

- The water droplets increase the electric field strength at the insulator surface because of their high permittivity and conductivity.
- The surface corona discharges from water droplets age the weather shed material of the insulator.
- The corona discharge destroys the hydrophobicity locally causing the spread of water, and adjacent water droplets to coalesce.

The corona discharge phenomena from water droplets have been investigated in recent publications [3, 4]. Phillips, Childs and Schneider studied the corona onset level and found that the typical electric field strength threshold value for the onset of water droplet corona lies between 5 to 7 kV/cm. Blackmore and Birtwhistle found that the discharges between water drops are characterized by a high cathode voltage fall and a physical structure similar to a low pressure glow discharge. The discharge produce localized loss of hydrophobicity on the polymer surface, which is predominantly caused by the cathode region of the discharge.

For the studies described in this paper, the commercially available program COULOMB based on the boundary element method, developed by Integrated Engineering Software, has been employed.

MODEL SETUP

As the first step, a simple model has been set up to study the basic features of the electric field distribution around a water droplet. For that purpose, a flat hydrophobic silicone rubber (SIR) sheet with a discrete water droplet is used to study the electric field enhancement in the vicinity of the water droplet. For further simplification, the single discrete water droplet is assumed to be hemispherical in shape.

Assuming a vertical suspension insulator, there are sessile water droplets on the sheds, and clinging water droplets on the

vertical surface of the polymer sheath of the insulator. The surface of the insulator shed is close to be parallel to the equipotential lines. The surface of the sheath is close to be perpendicular to the equipotential lines.

In order to represent the sheath region and the shed region, respectively, of an insulator, two electrodes are assumed together with the single SIR sheet. The size of the SIR sheet is 10 cm x 10 cm, and it is 0.5 cm thick. The relative permittivity of the SIR material used in the calculation is 4.3.

The two electrodes are positioned at 10 cm distance from each other. The SIR sheet is positioned in two different ways as shown in Figure 1. The sheath region is simulated by the SIR sheet positioned between the two electrodes as a spacer, shown by Figure 1(a). The SIR sheet is positioned parallel between the two electrodes for simulating the weather shed region, shown by Figure 1(b). In both cases, the applied voltage is 100 V, which means that the average electric field stress is about $100/10=10$ V/cm. A single water droplet (diameter 4mm, height 2mm) is assumed at midway of the electrode spacing. The relative permittivity of the water is 80.

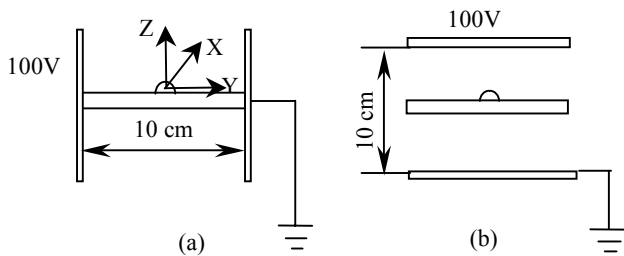


Figure 1 Experimental setup for simulation, (a) sheath region simulation, (b) shed region simulation.

ANALYSIS OF THE ELECTRIC FIELD ENHANCEMENT BY WATER DROPLETS

The hemispherical water droplet is modeled using 1500 elements. The enlarged view of the equipotential contours and electric field streamlines around the water droplet positioned on a SIR sheet simulating the sheath region, and the shed region, respectively, are shown in Figures 2 and 3. Continuous lines represent the equipotential lines; dashed lines are used for the electric field streamlines.

It can be seen from Figures 2 and 3 that the presence of the water droplet causes a considerable distortion in the configuration of the equipotential lines and electric field streamlines in the vicinity of the water droplet. For the sheath region simulation (Figure 2), the electric field strength is significantly increased at the interface of the water droplet, air, and the insulating material. For the shed region simulation

(Figure 3), the electric field strength is enhanced at the top of the water droplet.

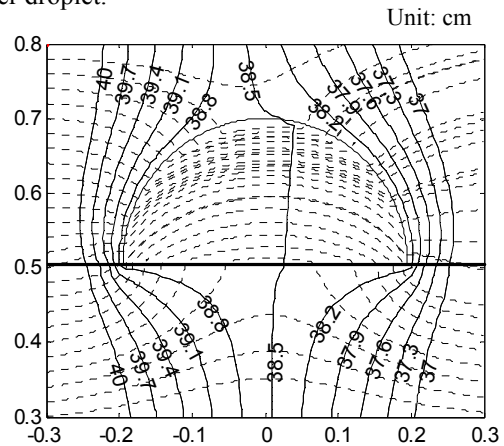


Figure 2. Equipotential contours and electric field streamlines around a water droplet simulating the sheath region.

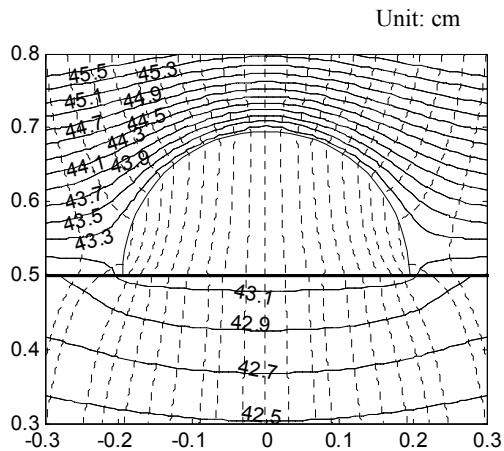


Figure 3. Equipotential contours and electric field streamlines around a water droplet simulating the shed region.

The electric field strength vector changes its magnitude and direction along the surface of the water droplet. To follow its changes, several quantities can be monitored, for example, the x, y, or z components of the electric field strength vector, or the magnitude of the vector.

The electric field strength magnitude on the surface of the water droplets on the sheath region and on the shed region, respectively, are shown by Figures 4 and 5. Each point on the surface of the water droplet is described by the three coordinates (x, y, z) of the location. In fact, a fourth dimension would be needed to show the distribution of the magnitude of the electric field strength. In order to be able to show the electric field strength distribution on the surface of the water droplet using a 3D graph, the surface point is represented by its (x, y) coordinates only. In other words, all points on the surface of the water droplet are represented by their projection in the (x, y) plane. Then the z dimension can be used to show

the magnitude of the electric field strength vector at any point on the surface of the water droplet.

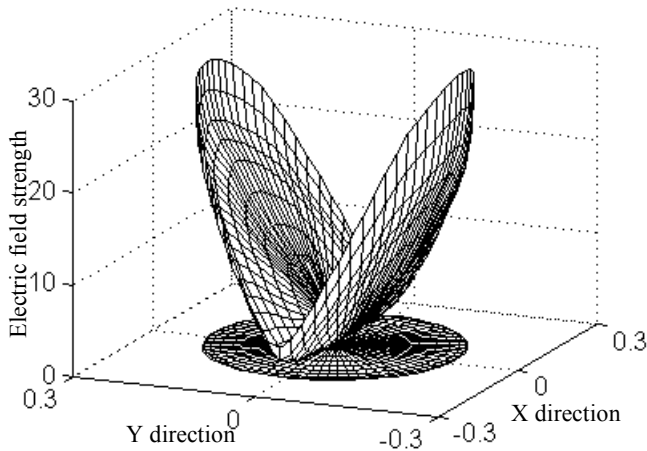


Figure 4. Electric field strength magnitude on the surface of the water droplet on the sheath region. X and Y directions are given in cm, the electric field strength is given in V/cm.

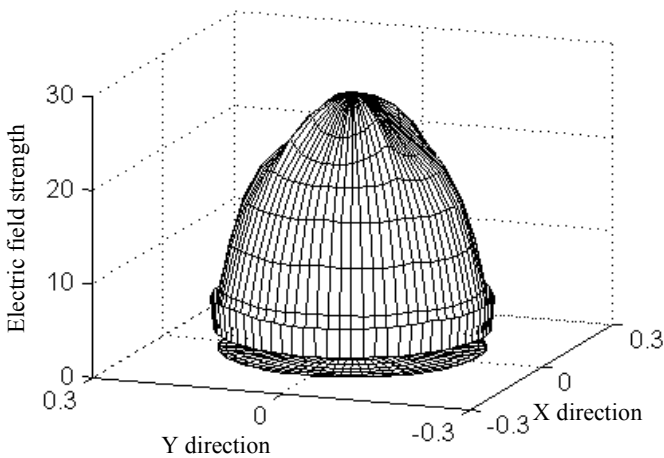


Figure 5. Electric field strength magnitude on the surface of the water droplet on the sheath region. X and Y directions are given in cm, the electric field strength is given in V/cm.

For a water droplet in the sheath region, the maximum value of the electric field strength is 29 V/cm (Figures 2 and 4), on the surface of the water droplet, at the interface of the water droplet, air and insulating material. For a water droplet in the shed region, the maximum value of the electric field strength is 27.6 V/cm (Figures 3 and 5) on the top of the water droplet. Zero water conductivity is considered for these cases.

If the relative permittivity and the conductivity of the water droplet are both considered, the maximum electric field strength values quoted above are modified. If the relative permittivity remains 80, and the conductivity is 250 $\mu\text{s/cm}$, the maximum value of the electric field strength is 35.5 V/cm for the water droplet in the sheath region and 31.7 V/cm in the

shed region, so the electric field enhancement further increases.

ANALYSIS OF THE POTENTIAL DISTRIBUTION UNDER RAIN AND FOG CONDITIONS

The test geometry considered for the following calculations is a short insulator with only four weather sheds. The simplified geometry and dimensions of the non-ceramic insulator to be modeled are shown in Figure 6.

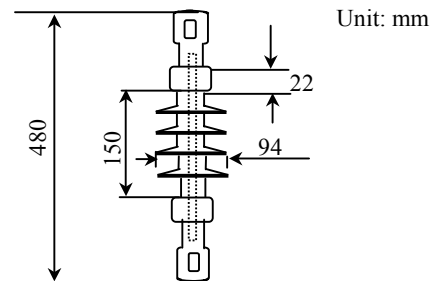


Figure 6. Geometry and dimensions of a four-shed non-ceramic insulator.

In order to reduce the calculation time, only a 10 degree segment of the weather shed surfaces is modeled. The applied voltage on the line end is 100 V.

The following three models are used for simulating specific weather conditions:

- The dry and clean model: the insulator identical to the shape of the non-ceramic insulator.
- The "rain" model: seven water droplets are assumed on each 10 degree segment of each weather shed. That means $7 \times 36 = 252$ water droplets on each shed, and $252 \times 4 = 1008$ water droplets on the four weather sheds of the insulator. The shape of all water droplets is hemispherical, with a diameter of 2mm. The relative permittivity of the water droplets is 80 and their conductivity is 50 $\mu\text{s/cm}$. The surface of the vertical sheath and the undersides of the sheds are dry.
- The "fog" model: the water droplet distribution is similar to that of the "rain" model, the only difference is that the undersides of the sheds are covered by a continuous water film layer. The relative permittivity of the water droplets is 80 and their conductivity is 250 $\mu\text{s/cm}$ for this case.

The equipotential contours of the three models are shown in Figure 7. Figure 7(a) shows (as expected) the non-uniform electric field distribution along a dry and clean insulator.

Figure 7(b) shows that assuming the "rain" model conditions, the electric field strength around the bottom weather shed area

is slightly less than in the dry and clean case. The presence of the water droplets on the top surface of the weather sheds makes the overall electric field distribution a bit more uniform than the dry case. (Of course, the local electric field strength in the vicinity of each water droplet is enhanced.) As a result, the overall electric field strength around the triple junction area (housing, air, and line-end metal fitting) will be a bit less than in the dry and clean case. Finally, Figure 7(c) shows that assuming the "fog" model conditions, the dry areas along the sheath sections of the insulator sustain most of the voltage. The overall electric field strength along the bottom area of the insulator is significantly higher than in the dry and clean case.

CONCLUSIONS

The electric field strength and potential distributions around the hemispherical water droplet have been calculated using the COULOMB software.

- The electric field strength is enhanced at the interface of the water drop, air and insulating material in the sheath region of the non-ceramic insulators. The degree of enhancement for the models considered is 2.9 to 3.5.
- The electric field strength is enhanced on the top of the water droplet on the shed region. The degree of enhancement for the models considered is 2.76 to 3.17.
- The overall electric field distribution along the insulator is more uniform for "rain" than for dry and clean conditions.

- The dry area along the sheath sections sustain most of voltage for the "fog" conditions assumed.

ACKNOWLEDGMENT

The support of Mr. Craig Armstrong, General Manager of Integrated Engineering Software, was invaluable for this study.

REFERENCES

1. De La O, A. and Gorur, R. S. "Flashover of Contaminated Non-Ceramic Outdoor Insulators in a Wet Atmosphere," IEEE Trans. Electrical Insulation, Vol. 5, No. 6, December 1998, pp. 814-823.
2. Gorur, R. S., De La O, A., El-Kishky, H., Chowdhury, M., Mukherjee, H., Sundaram R. and Burnham, J. T. "Sudden Flashover of Non-Ceramic Insulators in Artificial Contamination Tests," IEEE Trans. Electrical Insulation, Vol. 4, No. 1, February 1997, pp. 79-87.
3. Phillips, A. J., Childs, D. J., and Schneider, H. M. "Aging of Non-Ceramic Insulators due to Corona from Water Drops," IEEE Trans. Power Delivery, Vol. 14, No.3, July 1999, pp. 1081-1089.
4. Blackmore, P., and Birtwhistle, D. "Surface Discharge on Polymeric Insulator Shed Surfaces" IEEE Trans. Electrical Insulation, Vol. 4, No.2, April 1997, pp. 210-217.

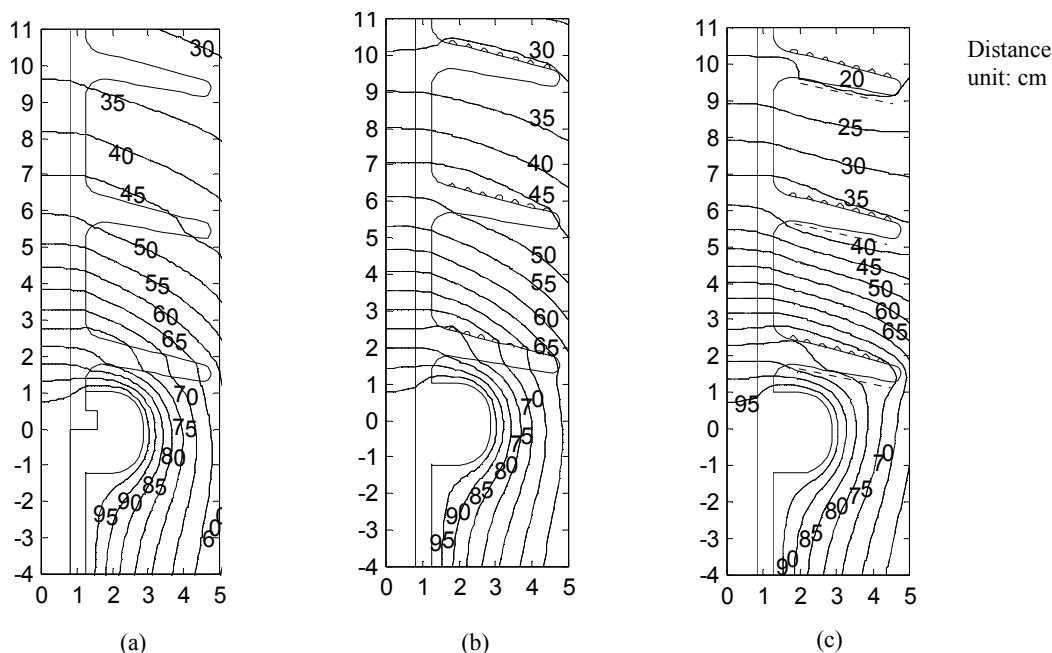


Figure 7 Equipotential contours for (a) dry and clean model (b) 'rain' model (c) 'fog' model